

# A Multidimensional NMR Experiment for Measurement of the Protein Dihedral Angle $\psi$ Based on Cross-Correlated Relaxation between $^1\text{H}^\alpha$ – $^{13}\text{C}^\alpha$ Dipolar and $^{13}\text{C}'$ (Carbonyl) Chemical Shift Anisotropy Mechanisms

Daiwen Yang,\*† Robert Konrat,‡ and Lewis E. Kay\*,†

Contribution from the Protein Engineering Network Centers of Excellence and Departments of Molecular and Medical Genetics, Biochemistry, and Chemistry, University of Toronto, Toronto, Ontario, Canada, M5S 1A8, and Institute of Organic Chemistry, University of Innsbruck, Innrain 52A, A-6060, Innsbruck, Austria

Received July 14, 1997<sup>§</sup>

**Abstract:** A high-resolution triple-resonance NMR method is presented for the measurement of the protein backbone dihedral angle  $\psi$  based on cross-correlated relaxation between  $^1\text{H}^\alpha$ – $^{13}\text{C}^\alpha$  dipolar and  $^{13}\text{C}'$  (carbonyl) chemical shift anisotropy relaxation mechanisms. The method relies on measurement of peak intensities of multiplet components in spectra recording zero- and double-quantum  $^{13}\text{C}^\alpha$ – $^{13}\text{C}'$  coherences. Results based on two proteins, ubiquitin and CheY, demonstrate a well-defined relation between cross-correlation rate and  $\psi$ .

## Introduction

Structure determination by NMR spectroscopy is largely predicated on the establishment of distance restraints, provided by the nuclear Overhauser effect between proximal proton pairs, and dihedral angle restraints, provided by scalar coupling constants between atoms separated by three bonds.<sup>1</sup> In the past several years, largely through the development of triple resonance multidimensional NMR spectroscopy, powerful new experiments have been designed for measurement of both distances and scalar couplings with high sensitivity and accuracy.<sup>2</sup> Very recently, Griesinger and co-workers have described an extremely elegant general strategy for the measurement of angles between interatomic bond vectors which does not require a predefined Karplus-type relation.<sup>3</sup> The approach is based on the use of cross-correlated relaxation between two separate relaxation interactions and has been demonstrated for the specific case of cross-correlation between inter-residue dipolar fields of  $^{15}\text{N}$ –NH (residue i) and  $^{13}\text{C}^\alpha$ – $^1\text{H}^\alpha$  (residue i-1) bond vectors to measure the protein backbone dihedral angle,  $\psi$ . Here we describe a second experiment for establishing the angle  $\psi$  which is based on measurement of cross-correlated relaxation between the  $^{13}\text{C}^\alpha$ – $^1\text{H}^\alpha$  dipolar interaction and the  $^{13}\text{C}'$  (carbonyl) chemical shift anisotropy relaxation mechanism. The present experiment offers significant sensitivity advantages over the dipole–dipole cross-correlation version and is demonstrated on the proteins ubiquitin (76 amino acids) and CheY (129 amino acids).

## Materials and Methods

Uniformly  $^{15}\text{N}$ , $^{13}\text{C}$ -labeled ubiquitin and CheY samples were kindly provided by Professors J. Wand, SUNY Buffalo, and R. Dahlquist, University of Oregon, respectively. Sample conditions were 2 mM protein, 50 mM potassium phosphate, pH 5.0, 90%  $\text{H}_2\text{O}$ /10%  $\text{D}_2\text{O}$ , 30 °C for ubiquitin and 1.8 mM protein, 5 mM  $\text{MgCl}_2$ , pH 6.8, 90%  $\text{H}_2\text{O}$ /10%  $\text{D}_2\text{O}$ , 30 °C for CheY. All spectra were recorded on a Varian UNITY+ 500 MHz spectrometer equipped with a pulsed field gradient

unit and a triple resonance probe with an actively shielded  $z$  gradient. Data sets consisting of  $60 \times 24 \times 512$  and  $50 \times 22 \times 512$  complex points were recorded for ubiquitin and CheY corresponding to acquisition times of (25.9 ms, 23.7 ms, 64 ms) and (23.9 ms, 21.7 ms, 64 ms) in each of ( $t_1$ ,  $t_2$ ,  $t_3$ ). A relaxation delay of 1 s was employed for both data sets resulting in net acquisition times of 13 h (ubiquitin; 4 scans/FID with an abridged phase cycle,  $T_C = 14$  ms) and 44 h (CheY; 16 scans/FID,  $T_C = 13$  ms). Spectra with  $(\phi_1, \phi_2)$  and  $(\phi_1 + \pi/2, \phi_2 + \pi/2)$  are recorded in an interleaved manner, and the data sets are added (subtracted) using in-house written software to generate  $^{13}\text{C}^\alpha$ – $^{13}\text{C}'$  zero- (double-) quantum spectra. All spectra were processed on SUN SparcStations using NMRPipe/NMRDraw<sup>4</sup> software and analyzed using CAPP/PIPP.<sup>5</sup> Mirror image linear prediciton<sup>6</sup> was employed to double the size of the  $t_1$  and  $t_2$  time domains according to the procedure outlined in Kay et al.<sup>7</sup> After processing the digital resolution (Hz/point) was 4.5, 4.0, 7.8 and 4.1, 4.0, 7.8 for spectra of ubiquitin and CheY.

## Results and Discussion

Figure 1 illustrates the pulse sequence that has been developed to measure relaxation interference between intraresidue  $^{13}\text{C}^\alpha$ – $^1\text{H}^\alpha$  dipolar and  $^{13}\text{C}'$  (carbonyl) chemical shift anisotropy (CSA) relaxation mechanisms. The experiment is analogous to the HN-(CO)CA scheme that has been published previously<sup>8</sup> in terms of the magnetization transfer steps, with the exception that  $^{13}\text{C}^\alpha$ – $^{13}\text{C}'$  zero- and double-quantum coherences evolve during the duration extending from points a to b in the figure. Note that this period is set to  $1/J_{CC}$ , where  $J_{CC}$  is the one-bond aliphatic carbon–carbon coupling, thereby minimizing the effects of one-bond carbon couplings on the sensitivity and resolution of the resultant spectrum.<sup>9,10</sup> However, use of this long delay presupposes that losses arising from  $^{13}\text{C}^\alpha$  transverse relaxation can be tolerated. Note that in cases where  $^{13}\text{C}^\alpha$  transverse relaxation times are prohibitively short it is possible to decrease the constant-time delay and refocus many of the

(4) Delagio, F.; Grzesiek, S.; Vuister, G. W.; Zhu, G.; Pfeifer, J.; Bax, A. *J. Biomol. NMR* 1995, 6, 277.

(5) Garrett, D. S.; Powers, R.; Gronenborn, A. M.; Clore, G. M. *J. Magn. Reson.* 1991, 95, 214.

(6) Zhu, G.; Bax, A. *J. Magn. Reson.* 1990, 90, 405.

(7) Kay, L. E.; Ikura, M.; Zhu, G.; Bax, A. *J. Magn. Reson.* 1991, 91, 422.

(8) Bax, A.; Ikura, M. *J. Biomol. NMR* 1991, 1, 99.

(9) Santoro, J.; King, G. C. *J. Magn. Reson.* 1992, 97, 202.

(10) Vuister, G. W.; Bax, A. *J. Magn. Reson.* 1992, 98, 428.

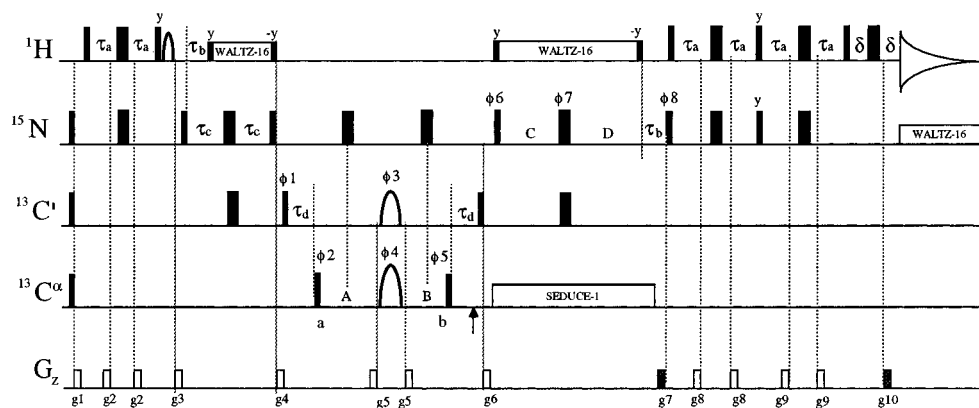


**Figure 1.** HN(CO)CA pulse scheme used to measure multiplet component intensities. All narrow (wide) pulses are applied with a flip angle of 90° (180°) and are along the  $x$ -axis, unless indicated otherwise. The  $^1\text{H}$ ,  $^{15}\text{N}$ , and  $^{13}\text{C}$  carrier frequencies are centered at 4.7 (water), 119, and 176 ppm, respectively.  $^{13}\text{C}^\alpha$  rectangular (shaped) pulses were applied at 58 ppm (50 ppm) by frequency shifting the rf.<sup>19,20</sup> All proton pulses are applied with a 33 kHz field with the exception of the water selective shaped pulse (90°) of duration 2 ms, the WALTZ-decoupling elements,<sup>21</sup> and the flanking pulses (6 kHz).  $^{15}\text{N}$  pulses use a 6.3 kHz field, while a 1 kHz decoupling field was employed. All carbon rectangular pulses were adjusted to a field strength of  $\Delta/\sqrt{15}$ , where  $\Delta$  is the separation between the centers of the  $^{13}\text{C}^\alpha$  and  $^{13}\text{C}'$  chemical shift regions.<sup>22</sup> The  $^{13}\text{C}'$  shaped pulses in the center of the carbon constant time evolution period have REBURP<sup>11</sup> ( $^{13}\text{C}^\alpha$ ; 400  $\mu\text{s}$ , 15.6 kHz peak rf) and r-SNOB<sup>23</sup> ( $^{13}\text{C}'$ ; 400  $\mu\text{s}$ , 5.8 kHz peak rf) profiles with the  $^{13}\text{C}^\alpha$  pulse applied prior to the  $^{13}\text{C}'$  pulse. Note that careful adjustment of the phases of both pulses must be done to ensure optimal sensitivity and proper  $F_1$  phasing. In some applications a  $^{13}\text{C}^\alpha$  Bloch-Siegert compensation pulse<sup>10</sup> (400  $\mu\text{s}$ , REBURP) was applied at the position indicated by the vertical arrow.  $^{13}\text{C}^\alpha$  decoupling during the  $^{15}\text{N}$  evolution period was achieved using WALTZ-16 with the shape of each of the elements (320  $\mu\text{s}$ ) given by the SEDUCE-1 profile.<sup>24</sup> The delays used are  $\tau_a = 2.3$  ms;  $\tau_b = 5.3$  ms;  $\tau_c = 12.4$  ms;  $\tau_d = 9.0$  ms;  $\delta = 0.5$  ms;  $A = T_c + t_1/2$ ;  $B = T_c - t_1/2$ ;  $C = T_N - t_2/2$ ;  $D = T_N + t_2/2 - \tau_b$ ;  $T_c = 13.0 - 14.0$  ms;  $T_N = 12.4$  ms. The phase cycling employed is  $\phi_1 = x, -x$ ;  $\phi_2 = y, -y, -y, y$ ;  $\phi_3 = 8(x), 8(-x)$ ;  $\phi_4 = 4(x), 4(-x)$ ;  $\phi_5 = 8(y), 8(-y)$ ;  $\phi_6 = x$ ;  $\phi_7 = 4(x), 4(-x)$ ;  $\phi_8 = x$ ;  $\text{rec} = 2(x), 2(-x), 2(x), 2(-x), 2(-x), 2(x)$ . A second spectrum is recorded (interleaved with the first) with  $\phi_1 = \phi_1 + \pi/2$ ,  $\phi_2 = \phi_2 + \pi/2$ . Data sets are added/subtracted to generate zero-/double-quantum spectra. Quadrature detection in  $F_1$  is achieved by States-TPPI<sup>25</sup> of  $\phi_2$ , while quadrature in  $F_2$  employs the enhanced sensitivity pulsed field gradient method,<sup>26,27</sup> where for each value of  $t_2$  separate data sets are recorded for  $(g7, \phi_8)$  and  $(-g7, \phi_8 + 180^\circ)$ . For each successive  $t_2$  value  $\phi_6$  and the phase of the receiver are incremented by 180°. The durations and strengths of the gradients are  $g1 = (0.5$  ms, 8 G/cm);  $g2 = (0.5$  ms, 5 G/cm);  $g3 = (1$  ms, 15 G/cm);  $g4 = (1$  ms, 10 G/cm);  $g5 = (0.4$  ms, 20 G/cm);  $g6 = (1$  ms, 15 G/cm);  $g7 = (1.25$  ms, 30 G/cm);  $g8 = (0.4$  ms, 5 G/cm);  $g9 = (0.3$  ms, 5 G/cm);  $g10 = (0.125$  ms, 29 G/cm).

$^{13}\text{C}^\alpha - ^{13}\text{C}^\beta$  couplings through the use of  $^{13}\text{C}^\beta$  selective (Iburp2<sup>11</sup>) inversion pulses applied concurrently with the  $^{15}\text{N}$  inversion pulses between points a and b. It is important to recognize that during the constant time carbon evolution period the one-bond heteronuclear  $^{13}\text{C} - ^1\text{H}$  coupling is operative, giving rise to spectra consisting of doublet and triplet multiplet components in the case of non-glycine and glycine residues, respectively. This is in contrast to the experiment which measures cross-correlation of  $^{15}\text{N}-\text{NH}$  and  $^{13}\text{C}^\alpha-^1\text{H}^\alpha$  dipolar fields in which two sets of doublets are observed for each correlation. In addition, the dipole/dipole cross-correlation experiment is affected by passive one-bond  $^{15}\text{N}-^{13}\text{C}^\alpha$  couplings involving both  $^{15}\text{N}$  and  $^{13}\text{C}^\alpha$  spins of either double- or zero-quantum coherences that are present during the carbon constant time period. This attenuates the signal by a factor of approximately 2.

Focusing for the moment only on  $^{13}\text{C}^\alpha-^1\text{H}^\alpha$  dipolar,  $^{13}\text{C}'$  CSA and  $^{13}\text{C}^\alpha$  CSA relaxation mechanisms and considering non-glycine residues it can be shown that the cross-correlation rate between  $^{13}\text{C}^\alpha-^1\text{H}^\alpha$  dipolar and  $^{13}\text{C}'$  CSA interactions,  $\Gamma_{\text{H}\alpha\text{C}\alpha,\text{C}'}$ , is given by<sup>12</sup>

$$1/(8T_C) \ln[(I_{D,2Q}I_{U,0Q})/(I_{D,0Q}I_{U,2Q})] = (4/15)(h/2\pi)\omega_C\gamma_C\gamma_H r_{\text{HC}}^{-3}\tau_C f(\sigma_X, \sigma_Y, \sigma_Z) \quad (1.1)$$

where

$$f(\sigma_X, \sigma_Y, \sigma_Z) = 0.5[\sigma_X(3\cos^2\theta_X - 1) + \sigma_Y(3\cos^2\theta_Y - 1) + \sigma_Z(3\cos^2\theta_Z - 1)] \quad (1.2)$$

In eq 1,  $I_{j,kQ}$  is the intensity of the upfield ( $j = \text{U}$ ) or downfield

( $j = \text{D}$ ) component of the multiplet in the spectrum recording  $k = (0,2)$  quantum coherences,  $\gamma_i$  is the gyromagnetic ratio of spin  $i$ ,  $r_{\text{HC}}$  is the distance between  $^1\text{H}^\alpha$  and  $^{13}\text{C}^\alpha$  nuclei,  $\tau_c$  is the correlation time describing overall tumbling of the assumed rigid and isotropically tumbling molecule,  $\omega_C$  is the carbon Larmor frequency,  $\sigma_i$  is the  $i$ th principal component of the chemical shift tensor, and  $\cos\theta_i$  is the direction cosine defining the orientation of the  $^{13}\text{C}^\alpha-^1\text{H}^\alpha$  bond with respect to the  $i$  axis of the carbonyl shift tensor. Note that the  $F_1$  frequencies of the D and U components are  $(\text{D}, \text{U}) = (\omega_C + \omega_{\text{Ca}} + \pi J_{\text{CH}}, \omega_C + \omega_{\text{Ca}} - \pi J_{\text{CH}}, -\omega_C + \omega_{\text{Ca}} + \pi J_{\text{CH}}, -\omega_C + \omega_{\text{Ca}} - \pi J_{\text{CH}})$  for the double- and zero-quantum coherences, respectively. The ratio of  $I_{j,kQ}$  values indicated in eq 1.1 ensures that contributions from auto-correlation relaxation, cross-correlation between  $^{13}\text{C}^\alpha-^1\text{H}^\alpha$  dipole and  $^{13}\text{C}^\alpha$  CSA, and cross-correlation between  $^{13}\text{C}^\alpha$  and  $^{13}\text{C}'$  CSA interactions are eliminated. Assuming standard bond lengths and angles, planar peptide bond geometry, and that the  $\text{Ca}-\text{C}'$  and  $\text{C}'-\text{N}$  bond vectors make angles of 22° and 38°, respectively, with respect to the X-axis of the principal C' chemical shift tensor frame,<sup>13</sup> the direction cosines can be recast in terms of the dihedral angle  $\psi$  according to

$$\cos\theta_X = -0.3095 + 0.3531 \cos(\psi - 120^\circ)$$

$$\cos\theta_Y = -0.1250 - 0.8740 \cos(\psi - 120^\circ)$$

$$\cos\theta_Z = -0.9426 \sin(\psi - 120^\circ) \quad (2)$$

In the case of glycine,  $\Gamma_{\text{H}\alpha\text{C}\alpha,\text{C}'}$  can be obtained by using the intensities of only the most upfield ( $I_U$ ) and most downfield

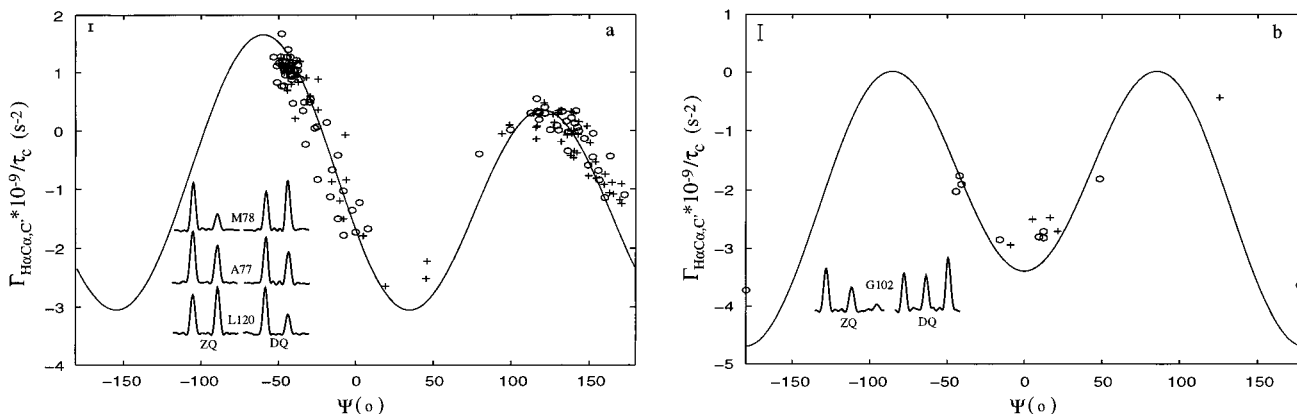


**Figure 2.** Correlation between calculated (solid line) and experimental values of  $\Gamma_{\text{H}\alpha\text{C}\alpha,\text{C}'}$  and  $\psi$  for non-glycine (a) and glycine (b) residues in ubiquitin (+) and CheY (o). Values of 244, 178, and 90 ppm were used for  $\sigma_X$ ,  $\sigma_Y$ , and  $\sigma_Z$ .<sup>13</sup> Average errors in  $\Gamma_{\text{H}\alpha\text{C}\alpha,\text{C}'}$  rates are shown by the vertical bars in the upper left hand corners. Several  $F_1$  cross sections from double- and zero-quantum spectra recorded on a sample of CheY (500 MHz  $^1\text{H}$  frequency) are illustrated.

( $I_D$ ) components of the triplet in eq 1.1 and substituting  $f(\sigma_X, \sigma_Y, \sigma_Z)$  with  $f_1(\sigma_X, \sigma_Y, \sigma_Z) + f_2(\sigma_X, \sigma_Y, \sigma_Z)$ , where  $f_1 = f$  and  $f_2$  is obtained by replacing  $(\psi - 120^\circ)$  with  $(\psi + 120^\circ)$  in eq 2.

Figure 2 illustrates a number of  $F_1$  cross sections from double- and zero-quantum spectra ( $^{13}\text{C}^\alpha - {^{13}\text{C}}'$ ) recorded on a sample of CheY. In addition, a plot of  $\Gamma_{\text{H}\alpha\text{C}\alpha,\text{C}'}/\tau_c$  as a function of  $\psi$  for 68 and 97 residues in ubiquitin (+) and CheY (o), respectively, is provided, superimposed on the theoretical curves generated from eqs 1 and 2 for the case of non-glycine (a) and glycine (b) residues. For both proteins  $\psi$  values were obtained from X-ray derived structures,<sup>14,15</sup> and previously published  $\tau_c$  values (4.0 ns and 7.8 ns for ubiquitin<sup>16</sup> and CheY<sup>17</sup>) were used. No attempt has been made to include the effects of internal dynamics. On average the correlation between experimentally derived cross-correlation rates and predicted values is very good. The average difference between  $\psi$  values calculated on the basis of measured values of  $\Gamma_{\text{H}\alpha\text{C}\alpha,\text{C}'}$  and  $\psi$  values established from the X-ray data for ubiquitin and CheY is  $6.5^\circ$  (non-glycine residues). Some scatter no doubt reflects the fact that ideal bond angles and lengths have been used, internal dynamics have been neglected, and that uniform values for both the components of the  $^{13}\text{C}'$  CSA tensor and the orientation of the tensor with respect to the molecular frame have been assumed.<sup>13</sup> In addition, in the analysis we have neglected contributions from an additional cross-correlation involving  $^1\text{H}^\alpha - {^{13}\text{C}}'$  dipolar and  $^{13}\text{C}^\alpha$  CSA mechanisms,  $\Gamma_{\text{H}\alpha\text{C}',\text{C}\alpha}$ . This term cannot be separated from  $\Gamma_{\text{H}\alpha\text{C}\alpha,\text{C}'}$ , and on the basis of published values for the  $^{13}\text{C}^\alpha$  CSA tensor<sup>18</sup> (which vary in a residue-specific manner) we estimate a maximum value of  $0.14 \text{ s}^{-2}$  for  $|\Gamma_{\text{H}\alpha\text{C}',\text{C}\alpha} * 10^{-9}/\tau_c|$ . Errors in estimated  $\psi$  values will depend on the magnitude of the  $^{13}\text{C}^\alpha$

(14) Vijay-Kumar, S.; Bugg, C. E.; Cook, W. J. *J. Mol. Biol.* **1987**, *194*, 531.

(15) Stock, A. M.; Martinez-Hackert, E.; Rasmussen, B. F.; West, A. H.; Stock, J. B.; Ringe, D.; Petsko, G. A. *Biochemistry* **1994**, *32*, 13375.

(16) Schneider, D. M.; Dellwo, M. J.; Wand, A. J. *Biochemistry* **1992**, *31*, 3645.

(17) Moy, F. J.; Lowry, D. F.; Matsumura, P.; Dahlquist, F. W.; Krywko, J. E.; Domaille, P. J. *Biochemistry* **1994**, *33*, 10731.

(18) Ye, C.; Fu, R.; Hu, J.; Hou, L.; Ding, S. *Magn. Res. Chem.* **1993**, *31*, 699.

(19) Patt, S. L. *J. Magn. Reson.* **1992**, *96*, 94.

(20) Boyd, J.; Scoffo, N. *J. Magn. Reson.* **1989**, *85*, 406.

CSA tensor (i.e., on  $\phi$  and  $\psi$ ). In the case of both proteins considered in the present study,  $\psi$  values are typically clustered in regions where  $\Gamma_{\text{H}\alpha\text{C}\alpha,\text{C}'}$  changes rapidly with  $\psi$ , and in most cases, errors introduced in  $\psi$  from neglect of the  $\Gamma_{\text{H}\alpha\text{C}',\text{C}\alpha}$  term are less than  $\pm 5^\circ$ . However, for  $\psi$  values of approximately  $-155^\circ$ ,  $-60^\circ$ ,  $35^\circ$ , and  $120^\circ$  for non-glycine residues and  $\pm 85^\circ$ ,  $\pm 180^\circ$ , and  $0^\circ$  for glycine, the errors can be on the order of  $\pm 10^\circ$ .

In summary a method for measuring  $\psi$  backbone dihedral angles in  $^{15}\text{N}$ ,  $^{13}\text{C}$  labeled proteins has been described and demonstrated for both ubiquitin and CheY. A good correlation is obtained between measured and predicted  $\Gamma_{\text{H}\alpha\text{C}\alpha,\text{C}'}$  values as a function of  $\psi$ , establishing the utility of the approach. Because multiplet components are restricted to doublets (or triplets for glycine) and passive couplings are refocused during delay times in the pulse scheme, sensitivity is sufficient for application to moderately sized proteins.

**Acknowledgment.** The authors are grateful to Professors J. Wand (SUNY, Buffalo) and Rick Dahlquist (Oregon) for kindly supplying  $^{15}\text{N}$ ,  $^{13}\text{C}$ -labeled samples of ubiquitin and CheY. This research was supported by the Natural Sciences and Engineering Research Council of Canada and the Medical Research Council of Canada. L.E.K. is an Alfred P. Sloan Fellow and an International Howard Hughes Research Scholar.

**Supporting Information Available:** A list of  $\Gamma_{\text{H}\alpha\text{C}\alpha,\text{C}'}$  values (and errors) for ubiquitin and CheY (5 pages). See any current masthead page for ordering and Internet access instructions.

JA972329Z

(21) Shaka, A. J.; Keeler, J.; Frenkel, T.; Freeman, R. *J. Magn. Reson.* **1983**, *52*, 335.

(22) Kay, L. E.; Ikura, M.; Tschudin, R.; Bax, A. *J. Magn. Reson.* **1990**, *89*, 496.

(23) Kupce, E.; Boyd, J.; Campbell, I. D. *J. Magn. Reson. Series B* **1995**, *106*, 300.

(24) McCoy, M.; Mueller, L. *J. Am. Chem. Soc.* **1992**, *114*, 2108.

(25) Marion, D.; Ikura, M.; Tschudin, R.; Bax, A. *J. Magn. Reson.* **1989**, *85*, 393.

(26) Kay, L. E.; Keifer, P.; Saarinen, T. *J. Am. Chem. Soc.* **1992**, *114*, 10663.

(27) Schleucher, J.; Sattler, M.; Griesinger, C. *Angew. Chem., Int. Ed. Engl.* **1993**, *32*, 1489.